



# Role of Ferumoxytol-enhanced MRI Imaging on HIV-Associated Cognitive Impairment

Baoxin "Hailey" Liang<sup>1</sup>, Dominic Chow<sup>2,3</sup>, Bronwyn Hamilton<sup>4</sup>, Jerod Rasmussen<sup>5</sup>, Chathura Siriwardhana<sup>3</sup>, Chieko Kimata<sup>6</sup>, Kalpana Kallianpur<sup>2,3</sup>, Cris Milne<sup>2</sup>, Debra Ogata-Arakaki<sup>2</sup>, Cecilia Shikuma<sup>2,3</sup>, Beau Nakamoto<sup>2</sup>

University of Rochester, Rochester, NY, USA<sup>1</sup>; Hawaii Center for AIDS, Honolulu, HI, USA<sup>2</sup>, John A. Burns School of Medicine, Honolulu, HI, USA<sup>3</sup>, Oregon & Health Science University, Portland, OR, USA<sup>4</sup>, University of California, Irvine, Irvine, CA, USA<sup>5</sup>, Hawaii Pacific Health, Honolulu, HI, USA<sup>6</sup>



## Introduction

Around 50% of HIV-infected individuals on combination antiretroviral therapy (cART) have cognitive impairment, more severe patients will develop HIV associated neurocognitive disorder (HAND).<sup>1</sup>

Limited information is known on the pathogenesis of HAND. One possible mechanism in which HAND develops is through HIV-infected monocytes/macrophages (M/MΦ) crossing the blood brain barrier, damaging neurons through the release of pro-inflammatory substances.<sup>2</sup> Our previous pilot study has shown that ferumoxytol-enhanced brain MRI demonstrates diffuse "tram track" appearances adjacent to the arterial and venous intracranial vessel walls of HIV+ individuals.<sup>3</sup>

Ferumoxytol is a small iron oxide MRI contrast agent.<sup>4</sup> "Tram track" appearances suggests the uptake of the small iron oxide MRI contrast agent by circulating monocytes.<sup>3</sup>

There is no "gold standard" quantitative neuroimaging modality capable of defining the extent of brain macrophage accumulation in individuals affected by HAND.

This project was a pilot study aimed to explore three MRI techniques with descriptive comparisons presented for each technique. It was hypothesized that ferumoxytol-enhanced QSM can be effectively used to quantitatively image the brain and an increase of iron concentration will be found in HIV+ subjects with neurocognitive impairment (NCI) in contrast to subjects without NCI.

## Materials and Methods

### Study Design

- This pilot study evaluated the MRI changes following ferumoxytol infusion between 3 study groups: HIV+Imp, HIV+, HIV-
  - 10 HIV+ subjects with NCI (HIV+Imp)
  - 10 HIV+ subjects (HIV+) and 10 seronegative (HIV-) subjects, both without NCI.
- Eligibility: 40-65 years old.
- Exclusions: no CVD, DM, HCV.
  - Further info. of exclusions found using NCT01665846
- Cognitive impairment was defined as a global z-score <-0.5 or a z-score <-0.5 in at least one cognitive domain known to be typically affected by HIV
- Neurocognitive assessment included tests of executive function, psychomotor speed and attention, working memory, and learning and memory
- MRI acquisitions were done on the same scanner for all subjects
- Quantitative susceptibility mapping (QSM), T2-Star (T2\*), T1-mapping measurements were obtained on pre- and post-ferumoxytol administrations.
- Differences between pre- and post-ferumoxytol MRI measures were calculated.

### Statistical Analysis

- Data shows the median of each brain region obtained by analysis of the delta visits. Delta calculated by Vist2(post) - Vist1(pre).
- P-values provided in the table represent group differences with respect to observed Delta values, by the Kruskal-Wallis test, separately under each technique (i.e., QSM, T1, T2\*) analyzed by IBM SPSS Statistics 25.0 (IBM Corp., Armonk, NY)
- QSM differences are set at a degree of 10<sup>-7</sup>.
- All P-values colored yellow indicate cases that are significant at 0.05 level; p-values colored green indicate cases that are significant at 0.1 level.

### MRI Acquisition

- MRI data was acquired on a 3.0 Tesla Philips Achieva scanner with an 8-channel head coil. MRIs were done at baseline and 3-5 days following ferumoxytol infusion.
- Whole-brain high-resolution anatomical T1-weighted image included a magnetization prepared rapid gradient echo sequence (MP-RAGE; T1-weighted volumes will include a sagittal T1-weighted 3D turbo field echo (T1W 3D TFE) sequence (echo time (TE)/repetition time (TR) = 3.1 ms/6.7 ms; flip angle (FA) = 8°; slice thickness 1.2 mm; no gap; in-plane resolution 1.0 mm<sup>2</sup>; field of view (FOV) = 256x256 mm<sup>2</sup>; scan time=10').
- QSM data was acquired using dual-echo 3D Gradient-Echo Sequence (TE<sub>1</sub>/TE<sub>2</sub>TR = 3/33/35ms; FOV = 220 mm; 130 transversal slices without gap; FA = 20°; scan time = 16'35"). The 30 ms TE difference was chose for high phase signal-to-noise ratio (SNR). Four echo times allowed for reconstruction of a T2\* map.
- T2 mapping data was acquired using a four-echo 3D Fast Field Echo (FFE) sequence (TR = 35ms; TE<sub>1</sub>/DeltaTE = 1.71/6.8 ms; 1x1x2 mm<sup>3</sup>voxels size; FOV = 220 mm; FA = 20°; scan time = 4'34").
- T1 mapping data was acquired using Two 3D FFE scans with FA = 5° and 15° (TE/TR = 1.6 ms; 1x1x2 mm<sup>3</sup>voxel size; FOV = 220 mm; scan time = 3'16" each).

### Ferumoxytol Administration

- Ferumoxytol infusion (dose of 4mg Fe/kg, up to max. 510 mg of elemental iron) delivered at rate of 1 ml/sec (30mg/sec) as a one-time infusion

### Quantitative MRI Analysis

#### Quantitative susceptibility mapping image processing

- Magnitude and phase images were reconstructed using FSL's BET, FNIRT, FLIRT tools.
- QSM processing was performed using the MEDI toolbox in Matlab.
- Reconstruction of the quantitative susceptibility maps utilized Morphology Enabled Dipole Inversion.

#### T2-Star Relaxometry image processing

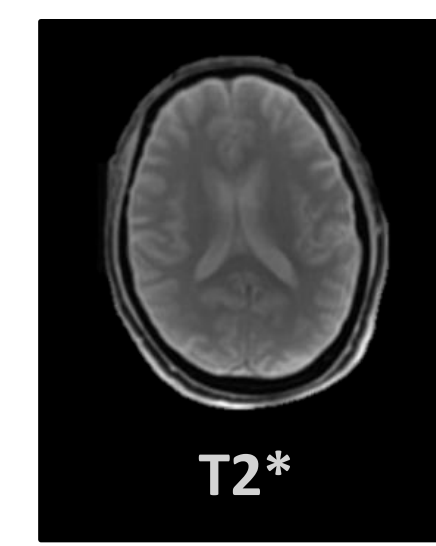
- T2-Star relaxometry measures determined using a dual-echo T2-star weighted acquisition.
- R2-star was empirically defined voxelwise using the ratio of the difference between the natural log transformed signal at TE<sub>1</sub> and TE<sub>2</sub> to the difference in TE
- T2-star was defined as the inverse of this value

#### T1 Relaxometry image processing

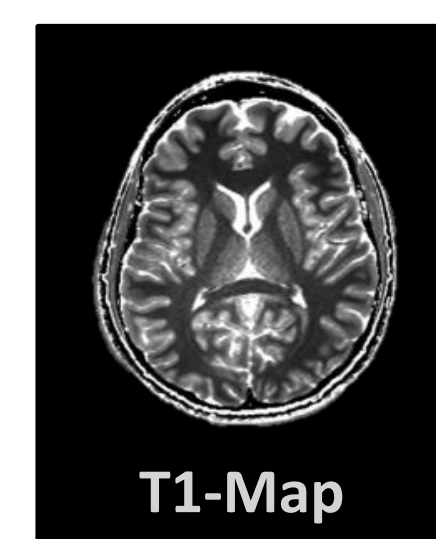
- T1-relaxometry measures were determined using a fast field echo with varying flip angle (FA=5 and 15 degrees) acquisition scheme
- T1 was empirically defined voxelwise using the signal ratio at varying flip angle and interpolated on a theoretically defined relationship between signal ratio and flip angle



QSM  
Chen et. al. 2018



T2\*  
Tang et. al. 2014



T1-Map  
Chen et. al. 2018

## Results

### Baseline Characteristics of Study Participants

	Group A: HIV- n=10	Group B: HIV+ n=10	Group C: HIV+Imp n=10	P-Value
Age	52.50 (51.57, 75)	54.50 (51.75, 57.75)	58.50 (53.25, 63.25)	0.261
Gender: Male	10 (100%)	10 (100%)	10 (100%)	
Ethnicity: Caucasian	6 (60%)	4 (40%)	5 (50%)	0.67
Education (years)	16.50 (14.00, 18.50)	15 (13.5, 18.5)	14 (12.75, 16.5)	0.314
Weight (kg)	192.0 (138.0, 225.50)	174.0 (133.0, 188.75)	172.0 (146.25, 192.5)	0.616
Height (cm)	172.72 (170.18, 184.47)	178.1 (168.9, 183.5)	173.67 (164.07, 180.66)	0.636
BMI	28.2 (21.63, 29.15)	25.5 (22.45, 27.2)	25.45 (24.23, 28.28)	0.581
Systolic pressure (mmHg)	116.50 (107.50, 127.50)	123.0 (110.0, 132.50)	112.0 (108.75, 129.75)	0.700
Diastolic pressure (mmHg)	72.50 (62.25, 83.50)	71.50 (64.75, 86.25)	72.5 (66.0, 74.0)	0.882
<b>Plasma Markers</b>				
Neopterin (nmol/L)	18.13 (15.22, 20.58)	21.28 (16.64, 38.49)	22.13 (19.33, 32.23)	0.108
S100B (pg/mL)	240.18 (222.93, 386.75)	233.91 (210.40, 272.37)	227.63 (198.65, 278.66)	0.077
sCD163 (ng/mL)	317.62 (293.92, 518.72)	472.84 (347.31, 655.56)	593.70 (460.77, 707.24)	0.476
<b>NP Z-scores</b>				
Global function	0.048 (-0.266, 0.593)Ψ	0.217 (0.119, 0.459)*	-0.577 (-1.115, -0.239)*Ψ	0.008*, 0.007Ψ
Executive function	0.048 (-0.110, 0.962)	0.829 (0.371, 1.120)*	-0.833 (-1.499, 0.358)*	0.013*
Learning and Memory	0.529 (-0.421, 0.962)	0.241 (-0.313, 1.046)	0.008 (-0.200, 0.795)	0.940
Working Memory	0.167 (-0.333, 0.236)	-0.056 (-0.333, 0.528)	-0.222 (-0.542, 0.167)	0.450
Psychomotor Speed	0.144 (-0.135, 0.740)	0.614 (0.261, 0.784)*	-0.561 (-1.044, 0.566)*	0.028*
CD4 count (cell/mL)	n/a	470.0 (374.25, 765.5)	568.0 (382.75, 697.5)	0.970
Nadir CD4 count (cell/mL)	n/a	69.0 (10.0, 211.25)	139.0 (4.75, 207.0)	0.705
HIV RNA < 50 copies/mL	n/a	10 (100%)	10 (100%)	-
<b>Smoking</b>				
Current Smoking	1 (10%)	2 (20%)	1 (10%)	1.000
<b>Alcohol</b>				
> 3 days use of Alcohol/week	4 (40%)	7 (70%)	9 (90%)	0.058
<b>Current Drug Use</b>				
Marijuana	0 (0%)	3 (30%)	4 (40%)	0.089
Cocaine	0 (0%)	0 (0%)	0 (0%)	-
Heroin	0 (0%)	0 (0%)	0 (0%)	-
Methamphetamine	0 (0%)	1 (10%)	0 (0%)	1.000
<b>Current Neurological Disorders</b>				
Seizures	0 (0%)	0 (0%)	0 (0%)	-
Depression	0 (0%)*	2 (20%)*	5 (50%)*	0.041*
Anxiety	1 (10%)	4 (40%)	4 (40%)	0.475
Others	0 (0%)	0 (0%)	1 (10%)	0.310
<b>Antiretroviral Medication</b>				
NRTI	n/a	10 (100%)	10 (100%)	-
NNRTI	n/a	2 (20%)	2 (20%)	-
PI	n/a	0 (0%)	4 (40%)	-
IN	n/a	7 (70%)	6 (60%)	-

Summary of n=30 patients, categorized by HIV groups. Categorical variables were summarized with frequencies and percentages. Continuous variables were given by medians (Q1, Q3).

### Ferumoxytol Group Differences in MRI Techniques

Brain Region	QSM	QSM P-Value	T2*	T2* P-Value	T1-Mapping	T1-Mapping P-Value	
Gray Matter	HIV+Imp	3.14	0.146	HIV+Imp -3.42	0.043*	HIV+Imp -6.3	0.038*
	HIV+	-2.66		HIV+ -7.68		HIV+ -96.35	
Corpus callosum	HIV+Imp	-14.8	0.026*	HIV+Imp -1.87	0.251	HIV+Imp 16.60	0.066
	HIV+	-100		HIV+ -4.14		HIV+ -45.45	
Splenium	HIV+Imp	-43.8	0.564	HIV+Imp -1.01	0.533	HIV+Imp -113.99	0.024*
	HIV+	-7.93		HIV+ -3.44		HIV+ -11.99	
Corpus callosum body	HIV+Imp	0.670	0.252	HIV+Imp -2.34	0.939	HIV+Imp 24.53	0.149
	HIV+	-27.2		HIV+ -3.00		HIV+ -26.27	
Corpus callosum genu	HIV+Imp	-72.4	0.898	HIV+Imp -1.61	0.141	HIV+Imp 23.00	0.062
	HIV+	-47.3		HIV+ -2.90		HIV+ -50.65	
Corpus callosum	HIV+Imp	-30.6	0.742	HIV+Imp -2.26	0.029*	HIV+Imp -106.81	0.158
	HIV+	-35.5		HIV+ -4.11		HIV+ -136.10	
Brainstem	HIV+Imp	-186.0	0.324	HIV+Imp -3.52	0.018*	HIV+Imp -8.20	0.052
	HIV+	-165.0		HIV+ -7.93		HIV+ -69.75	
Frontal Gray Matter	HIV+Imp	-14.6	0.922	HIV+Imp -16.6	0.050	HIV+Imp -122.80	0.042*
	HIV+	-9.23		HIV+ -7.33		HIV+ -94.75	
Temporal Gray Matter	HIV+Imp	-2.19	0.311	HIV+Imp -2.95	0.072	HIV+Imp -110.20	0.060
	HIV+	-18.7		HIV+ -5.94		HIV+ -157.55	
Occipital Gray Matter	HIV+Imp	-70.5	0.221	HIV+Imp -5.81	0.135	HIV+Imp -283.85	0.080
	HIV+	-18.0		HIV+ -4.67		HIV+ -22.50	
Parietal Gray Matter	HIV+Imp	8.53	0.214	HIV+Imp -4.13	0.122	HIV+Imp -15.00	0.101
	HIV+	-21.0		HIV+ -8.00		HIV+ -90.40	
Cerebellum Gray Matter	HIV+Imp	16.3	0.524	HIV+Imp -8.21	0.298	HIV+Imp -200.60	0.146
	HIV+	-14.2		HIV+ -15.07		HIV+ -689.10	
Subcortical Gray Matter	HIV+Imp	62.0	0.691	HIV+Imp -2.05	0.231	HIV+Imp 17.45	0.082
	HIV+	-339.0		HIV+ -4.09		HIV+ -37.36	
Frontal White Matter	HIV+Imp	-30.2	0.811	HIV+Imp -2.48	0.289	HIV+Imp 49.60	0.054
	HIV+	-28.8		HIV+ -4.30		HIV+ -45.11	
Temporal White Matter	HIV+Imp	-41.9	0.054	HIV+Imp -3.77	0.080	HIV+Imp -96.12	0.106
	HIV+	-61.6		HIV+ -2.29		HIV+ -25.86	
Occipital White Matter	HIV+Imp	-141.0	0.344	HIV+Imp -4.64	0.206	HIV+Imp -43.67	0.076
	HIV+	-72.1		HIV+ -4.34		HIV+ -97.65	
Parietal White Matter	HIV+Imp	-16.8	0.330	HIV+Imp -2.47	0.104	HIV+Imp 11.76	0.080
	HIV+	-59.8		HIV+ -2.85		HIV+ -41.48	
Cerebellum White Matter	HIV+Imp	-37.7	0.361	HIV+Imp -3.64	0.158	HIV+Imp 6.80	0.089
	HIV+	-29.3		HIV+ -7.44		HIV+ -62.45	
Supratentorial White Matter	HIV+Imp	39.6	0.222	HIV+Imp -5.01	0.089	HIV+Imp -134.00	0.054
	HIV+	-20.1		HIV+ -2.14		HIV+ -33.74	
Intracranial	HIV+Imp	-48.8	0.260	HIV+Imp -4.28	0.089	HIV+Imp -79.21	0.054
	HIV+	-32.8		HIV+ -4.01		HIV+ -97.21	
Whole Brain	HIV+Imp	-9.59	0.260	HIV+Imp -3.14	0.089	HIV+Imp -11.80	0.054
	HIV+	-19.3		HIV+ -6.33		HIV+ -75.10	
Whole Brain	HIV+Imp	-0.72	0.260	HIV+Imp -5.93	0.089	HIV+Imp -182.2	0.054
	HIV+	-12.1		HIV+ -2.87		HIV+ 8.80	
Whole Brain	HIV+Imp	-27.0	0.260	HIV+Imp -5.71	0.089	HIV+Imp -53.70	0.054
	HIV+	-7.38		HIV+ -5.48		HIV+ -149.66	

## Conclusion

- This is the first study that quantifies ferumoxytol-enhancement in the HIV population
- QSM:**
  - There were few differences in ferumoxytol-enhanced QSM imaging in the three groups.
  - Currently, this technique may not be sensitive enough to detect post-ferumoxytol brain differences.
  - i.e. signal to noise differences in the brain are not large enough to detect changes
- T2\*:**
  - There were varying degrees of change, but no observable trend in enhancement.
- T1-mapping:**
  - There was an incremental increase in degrees of ferumoxytol-related enhancement on T1-mapping.
  - Change was greatest in HIV-infected subjects with cognitive impairment.
- Future studies:**
  - Associations between T1-mapping in Ferumoxytol-enhanced brain MRI and inflammatory markers is an area of future exploration.
- Limitations:**
  - Limitations to this research include a small sample size and a lack of a "gold standard" MRI method for quantification.

## References

- Heaton RK, Clifford DB, Franklin JD R., Woods SP, Ake C, Vaida F, et al. HIV-associated neurocognitive disorders persist in the era of potent antiretroviral therapy: CHARTER Study. Neurology. 2010;75(23):2087-96.
- Koenig S, Gendelman HE, Orenstein JM, Canto MC, Peshkpor GH, Yungbluth M, et al. Detection of AIDS Virus in Macrophages in Brain Tissue from AIDS Patients with Encephalopathy. Science. 1986;233(4768):1089-93.
- Nakamoto BK, Shikuma CM, Ogata-Arakaki D, Umaki T, Neuwelt EA, Shiramizu BT, et al. Feasibility and potential role of ferumoxytol-enhanced neuroimaging in HIV-associated neurocognitive disorder. J Neurovirol. 2013;19(6):601-5.
- Neuwelt EA, Hamilton BE, Varallyay CG, Rooney WR, Edelman RD, Jacobs PM, et al. Ultrasmall superparamagnetic iron oxides (USPIOs): a future alternative magnetic resonance (MR) contrast agent for patients at risk for nephrogenic systemic fibrosis (NSF)? Kidney Int. 2009;75(5):465-74.

## Acknowledgements

The authors thank the study participants and InVision for their assistance. This work was supported by NIH NINDS R21NS087951, and the Queen's Summer Research Internship